JOURNAL OF APPLIED ELECTROCHEMISTRY 18 (1988) 323–332

A voltammetric study of galena immersed in acetate solution at pH 4.6

M. D. PRITZKER*, R. H. YOON

Department of Mining and Minerals Engineering, Virginia Polytechnic Institute and State University, Blacksburg, Virginia 24061, USA

Received 24 December 1986; revised 7 August 1987

The electrochemistry of galena in an acetate solution at pH 4.6 has been studied through the use of linear sweep voltammetry. Analysis of the voltammograms for anodic limits as high as 845 mV indicates that S^0 is the sulphur-bearing species generated during the oxidative dissolution of galena. Furthermore, interpretation of the electrochemical data on the basis of thermodynamic considerations indicates that galena interacts with the acetate electrolyte and that $Pb(CH_3COO)_2(aq)$ is also produced during anodic oxidation. When the scan direction is reversed in the cathodic direction, the oxidation products are removed by two reduction reactions when the solution is quiescent: the recombination of $Pb(CH_3COO)_2$ and S^0 to form PbS and the reduction of S^0 to H_2S. In a stirred solution, only the second reaction is possible. Experiments conducted in the presence of 10^{-3} or 10^{-2} M lead acetate indicate that the presence of dissolved lead tends to inhibit the dissolution process. Furthermore, metallic lead can begin to deposit on the galena surface when the potential drops below about −330 mV SHE. The data also agree most closely with thermodynamics when $Pb(CH_3COO)_2$ is considered to be the aqueous species involved in the deposition and dissolution of metallic lead.

1. Introduction

Over the years, galena has proved to be one of the sulphide minerals most widely studied by metallurgists, geochemists and electrochemists alike. Some of this interest stems from the richness and complexity of the aqueous chemistry of this mineral and of sulphides in general. An understanding of the behaviour of galena also has great practical importance since it is the principal source of metallic lead. Unlike the case of most other sulphides, the chemical extraction of this metal on a commercial level is carried out exclusively via the pyrometallurgical route. Nevertheless, there has been a great deal of effort to develop hydrometallurgical processes for the recovery of lead, e.g. [1–9]. Some of the most recent attention has been focused on the use of ferric chloride to leach galena [5–9].

Since all such processes invariably involve electron transfer reactions, the electrochemistry of these systems is central to the description of what occurs. Several electrochemical studies on galena in acidic media which have been reported include the work of Brodie [10], Eadington and Prosser [11], Springer [12], Paul *et al.* [13], Johnson *et al.* [14], Gardner and Woods [15], Lamache *et al.* [16] and Sivenas and Foulkes [17]. However, certain questions still remain and various aspects need to be explored further.

Perhaps the most extensive voltammetric studies of galena have been those conducted by Paul *et al.* [13] and Gardner and Woods [15]. They examined its anodic and cathodic behaviour in a variety of buffer solutions over a pH range between 1 and 13. In this paper, we focus our attention on one of the electrolytes that Gardner and Woods used (0.5 M CH_3COOH/0.5 M CH_3COONa at pH 4.6) and look at the voltammetric behaviour of lead sulphide in more detail. The choice of this electrolyte is quite interesting since, not only does it act as a pH buffer and control the ionic strength, but the acetate anion is also capable of forming complexes with lead. As will be shown, this may have an effect on the electrochemistry of the mineral.

It is inevitable that, in any environment where galena is quite soluble, the mineral chemistry will begin to reflect the influence of the accumulation of dissolved lead in solution. In order to examine this more closely, we include in our study experiments in which excess lead (10^{-3} and 10^{-2} M) in the form of lead acetate is added to the electrolyte.

2. Experimental details

The galena sample used in this work was a research grade (>99% pure) specimen originating from Brushy Creek, Missouri, and was obtained from Ward's Natural Science Establishment. An electrode was prepared by cutting a piece, approximately 1 cm in length and 0.65 cm^2 in cross-sectional area, and permanently attaching a copper lead to the back of the specimen using a carbon-based conducting cement, Electrodag 199. This assembly was then sealed in a glass holder with Buehler epoxy resin.

All the tests were carried out at pH 4.6 in 0.5 M CH_3COOH/0.5 M CH_3COONa (ACS grade) solutions.

---

* *Present Address*: Department of Chemical Engineering, University of Waterloo, Waterloo, Ontario, Canada N2L 3G1.

0021-891X/88 $03.00 + .12

Prior to a series of experiments, the electrolyte was deoxygenated by purging with low-oxygen nitrogen (< 0.5 p.p.m. O_2) for at least 1 h. The gas sparger was raised above the top of the solution at the start of an experiment and nitrogen was continually introduced to maintain a positive pressure thereafter. Upon the completion of a test, the electrode was removed from the reaction vessel, polished with 400- and 600-grit silicon carbide paper, rinsed with distilled water and placed back onto the cell for the next experiment.

A conventional three-electrode system was used during the voltammetry experiments. The electrode potential was controlled using a PAR Model 371 potentiostat/galvanostat and a PAR Model 175 waveform generator, and the current response was monitored on a Hewlett Packard 7004B X-Y recorder. All potentials were measured against a saturated calomel reference electrode, although the data presented here have been converted to the standard hydrogen scale.

3. Results and discussion

A series of voltammetry experiments was run to investigate the sequence of electrochemical reactions occurring on a polarized galena electrode immersed in an acetate solution at pH 4.6.

3.1. *Identification of peaks*

Fig. 1 shows the voltammograms obtained in stirred and unstirred solutions for an anodic limit of 645 mV and a cathodic limit of -755 mV. The results show clearly that stirring increases the oxidation rate of galena. Determination of the area under both voltammograms in Fig. 1 indicates that a balance between the anodic and cathodic charges exists. This observation suggests that elemental sulphur rather than thiosulphate or sulphate, which tends to form irreversibly, is being generated during oxidation. Similar results have been reported by Gardner and Woods [15] and Lamache *et al.* [16].

Identification of the lead-bearing oxidation product is complicated by the fact that lead can readily form complexes with the acetate electrolyte. Although Gardner and Woods [15] used the same buffer in their study, they did not consider the possibility of lead complex formation in the analysis of their data. In order to obtain a better idea of which species are being produced, it is instructive to carry out some calculations of the thermodynamics of the lead/acetate system under the conditions of these experiments. The free-energy values for the various species considered have been determined from data presented by Martell and Smith [18] and are given in Table 1. Deviations from ideal behavior have been taken into account by using the Davies equation [19] to calculate the activity coefficient, γ_i, of a given ionic species:

$$\log \gamma_i = -Az_i^2\left(\frac{I^{1/2}}{1 + I^{1/2}} - 0.2I\right) \qquad (1)$$

where A is a constant which depends on temperature and solvent ($A = 0.51$ for water at 25° C), z_i is the valence of the ion and I is the ionic strength of the solution.

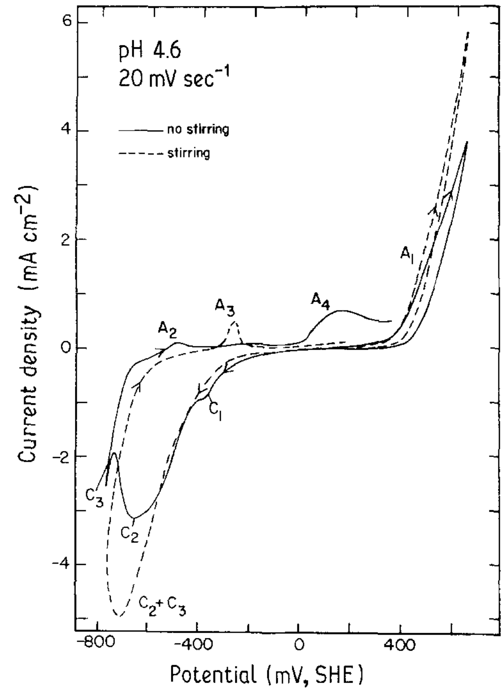

Fig. 1. Effect of stirring on the single sweep voltammograms for a galena electrode immersed in a 0.5 M CH_3COOH/0.5 M CH_3COONa solution (pH 4.6). Potential scan between -755 and 645 mV. Scan rate = 20 mV sec^{-1}.

A_1 = PbS, CH_3COO^-/$Pb(CH_3COO)_2$, S^0
A_2 = Pb^0, H_2S/PbS
A_3 = Pb^0, CH_3COO^-/$Pb(CH_3COO)_2$
A_4 = H_2S/S^0
C_1 = $Pb(CH_3COO)_2$, S^0/PbS, CH_3COO^-
C_2 = S^0/H_2S
C_3 = PbS/Pb^0, H_2S

With this information, we can calculate the molar ratios of the various species in the electrolyte containing 0.5 M CH_3COOH/0.5 M CH_3COONa at pH 4.6 (Table 2). The results indicate that virtually all of the soluble lead present should be in the form of a lead acetate complex and, furthermore, that $Pb(CH_3CO_2)_2$ should be the most abundant species. On the basis of this consideration, one might expect that the oxidation of galena occurs primarily by the reaction,

$$PbS + 2CH_3COO^- \longrightarrow Pb(CH_3COO)_2(aq) + S^0 + 2e^-, \qquad (2)$$

during the anodic scan in Fig. 1. The Nernst potential

Table 1. Free energy data for species considered in the lead/acetate system at $T = 298°$ C and $P = 1$ atm.

	ΔG_f^0 (*kcal mol*$^{-1}$)
Pb^{2+}	-5.81
CH_3COO^-	-89.02
CH_3COOH	-95.51
$PbCH_3COO^+$	-98.48
$Pb(CH_3COO)_2$	-189.41
$Pb(CH_3COO)_3^-$	-278.28
$Pb(CH_3COO)_4^{2-}$	-365.94

Table 2. Equilibrium molar ratios for lead/acetate system in 0.5 M CH_3COOH/0.5 M CH_3COONa electrolyte at pH 4.6

$[PbCH_3COO^+]/[Pb^{2+}]$	54.7
$[Pb(CH_3COO)_2]/[Pb^{2+}]$	328.4
$[Pb(CH_3COO)_3^-]/[Pb^{2+}]$	127.5
$[Pb(CH_3COO)_4^{2-}]/[Pb^{2+}]$	13.3

for this reaction is 104 mV SHE [18], assuming the concentration of $Pb(CH_3COO)_2$ to be 10^{-6} M.

Upon reversal of the scan in the cathodic direction, a small peak, C_1, and a much larger one, C_2, appear at −400 and −600 mV, respectively, when the solution is unstirred. However, if the electrolyte is agitated, C_1 disappears and only C_2 remains. A similar observation has been reported by Gardner and Woods [15]. This suggests that the smaller peak at C_1 is associated with a reaction in which a soluble species generated during the previous anodic scan participates. Presumably, this is simply the reverse of the anodic reaction at A_1, i.e.,

$$Pb(CH_3COO)_2(aq) + S^0 + 2e \longrightarrow PbS + 2CH_3COO^-. \qquad (3)$$

The process occurring at C_2 probably involves the reduction of an insoluble oxidation product since it takes place regardless of the stirring conditions and can therefore be identified with the reaction,

$$S^0 + 2H^+ + 2e \longrightarrow H_2S, \qquad (4)$$

which has a reversible potential of 47 mV [18] at pH 4.6, assuming $[H_2S] = 10^{-6}$.

Although Gardner and Woods [15] did not consider the possibility of lead complex formation in their study, their discussion concerning the relationship between the reactions occurring during the cathodic scan still applies. Both reactions (3) and (4) proceed under quiescent conditions since some $Pb(CH_3COO)_2$ will always diffuse away from the electrode surface by the time the potential scan is reversed in the negative direction and the cathodic reactions can occur. The result of this stoichiometric excess of S^0 over $Pb(CH_3COO)_2$ is that direct reduction of S^0 according to (4) is necessary for all of the oxidation product to be removed. Another contributing factor may be that reaction (3) is slow enough that reaction (4) occurs even if some $Pb(CH_3CO_2)_2$ is still present at the surface.

As the scan continues beyond the two peaks at C_1 and C_2, a third peak, C_3, due to the cathodic decomposition of galena, i.e.,

$$PbS + 2H^+ + 2e \longrightarrow Pb^0 + H_2S \qquad (5)$$

appears. In the unstirred case, there is some separation between the current rise for this reaction and that for C_2. However, when the solution is stirred, there is so much oxidation of the mineral during the previous anodic scan that C_2 and C_3 probably overlap.

The voltammograms in Fig. 1 also show that stirring has a significant effect once the sweep is continued further and reversed back in the anodic direction for the second time. Two peaks, A_2 and A_4, appear when the solution is quiescent, whereas only a single peak, A_3, is observed under stirred conditions. This suggests that H_2S, which is produced by reactions (4) and (5) during the previous cathodic sweep, participates in A_2 and A_4, but not in A_3. Reasonable choices for the first two of these reactions are:

$$A_2 \quad Pb^0 + H_2S \longrightarrow PbS + 2H^+ + 2e \qquad (6)$$

$$A_4 \quad H_2S \longrightarrow S^0 + 2H^+ + 2e \qquad (7)$$

It should also be noted that the calculated Nernst potentials [18] for (6) and (7) are −454 and 47 mV, respectively (assuming $[H_2S] = 10^{-6}$ M), and lie quite close to where the peaks, A_2 and A_4, begin to rise in Fig. 1.

The process associated with A_3, on the other hand, probably involves the oxidation of the insoluble species (Pb^0) generated during the cathodic scan according to,

$$A_3 \quad Pb^0 + 2CH_3COO^- \longrightarrow Pb(CH_3COO)_2 + 2e \qquad (8)$$

This is supported by the fact that the equilibrium potential for this reaction of −395 mV [18] under the conditions of 10^{-6} M $Pb(CH_3COO)_2$ and 0.5 M CH_3COO^- agrees well with the position of A_3. It is also interesting to note that A_3 does not appear in the unstirred case, although reaction (8) should still be possible. One reason for this may be that all the elemental lead produced on the electrode surface by reaction (5) has been removed by reaction (6) at A_2.

Because of the separation between C_3 and the other two cathodic peaks in the quiescent case, it is possible to estimate the cathodic charge associated with the removal of the oxidation products from the first anodic scan and compare it to the anodic charge passed. From the voltammogram shown in Fig. 1, it has been determined that 45.5 mC/cm^2 of charge is passed during oxidation, whereas 45.0 mC/cm^2 is consumed during reduction. This balance is consistent with what would be anticipated if (2), (3) and (4) are, indeed, the reactions involved.

In order to estimate the charges in the stirred case, a different approach has been taken because of the overlap of the reduction peaks. If all of the Pb^0 produced by the reduction of PbS is oxidized to $Pb(CH_3COO)_2$ at A_3, then the anodic charge associated with the latter reaction can be used as a measure of how much of the cathodic charge is associated with C_3. Since all the reactions involve the transfer of 2 F gmol^{-1} of lead reacted, the charge for C_2 should be equal to the difference between the total cathodic charge passed (including the anodic-going portion) and the anodic charge due to A_3. Analysis of the voltammogram using this approach indicates that the charge due to C_2 is 72.6 mC/cm^2, compared to the value of 71.2 mC/cm^2 for the oxidation of PbS on the first scan. Considering some of the inaccuracies with this method, it appears that a charge balance exists.

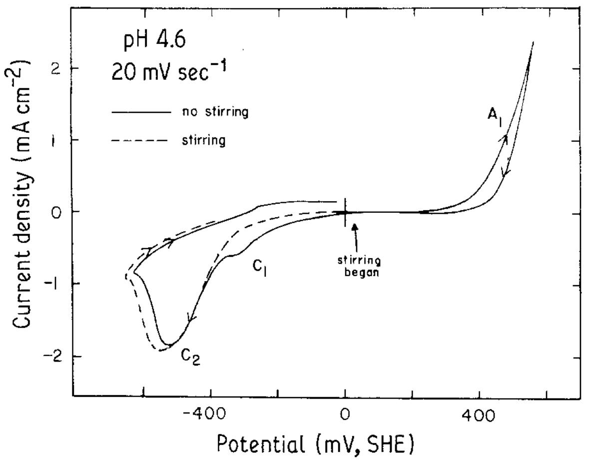

Fig. 2. Effect of stirring on the cathodic portion of the single sweep voltammograms for a galena electrode immersed in a 0.5 M CH_3COOH/0.5 M CH_3COONa solution (pH 4.6). Potential scan between −625 and 545 mV. Scan rate = 20 mV sec^{-1}.

A_1 = PbS, $CH_3COO^-/Pb(CH_3COO)_2$, S^0
C_1 = $Pb(CH_3COO)_2$, S^0/PbS, CH_3COO^-
C_2 = S^0/H_2S

Previously, Gardner and Woods [15] had proposed that the direct reduction of S^0 and H_2S occurs because there is always an excess of S^0 over Pb^{2+} near the electrode surface whether the solution is being agitated or not. Thus, the complete disappearance of the C_1 peak under stirred conditions at pH 4.6 (Fig. 1) results from the total removal of Pb^{2+} ions from the mineral surface. We carried out the following experiment to look at this question more closely. The potential was swept to an upper limit of 545 mV before being reversed and reduced to about −625 mV in order to completely remove all the oxidation products. The electrolyte was left unstirred throughout this scan. This was followed by a second scan which was identical to the first in every respect except that stirring was begun when the potential reached a value of about 50 mV during the cathodic-going portion of the sweep (Fig. 2).

As can be seen, stirring causes the C_1 peak to disappear, although the conditions under which galena has been oxidized and the resulting electrode response are exactly the same in both scans. This result does support the interpretation proposed by Gardner and Woods [15]. Integration of the voltammograms indicates that the loss of 1.2 mC resulting from the disappearance of C_1 in the stirred case is exactly compensated by a 1.2 mC enlargement of C_2.

The information obtained from this experiment can also be used to estimate the relative amounts of current consumed by reactions (3) and (4) under quiescent conditions. The charge passed during the oxidation of the mineral is determined to be 7 mC. Assuming that all the oxidation products are removed by the time the cathodic limit is reached, then the fraction of the current due to reaction (4) is 1.2/7.0 or 0.17. This shows that even under relatively quiescent conditions, the reduction of S^0 to H_2S (reaction (2)) is the predominant cathodic reaction. Evidently, a considerable amount of $Pb(CH_3COO)_2$ has diffused away by the time reduction commences and/or the kinetics of reaction (3) are slower than those of reaction (4).

3.2. *Effect of anodic limit*

The effect on the voltammograms of varying the anodic limit from 445 to 845 mV is shown in Fig. 3. These experiments were carried out at a scan rate of 20 mV sec^{-1} in a stirred solution. The cathodic limit in each case was extended far enough to ensure that all the oxidation products were removed.

At the two highest anodic limits, a peak in the anodic rise at A_1 appears at approximately 650 mV, followed by a minimum at about 700 mV. Similar behavior has been observed by others at this and other pH values [13, 15]. It may be due to the fact that the initial sulphur layer formed during the scan inhibits further oxidation. Enough has accumulated by 650 mV to cause the current to drop until the potential is raised by another 50 mV.

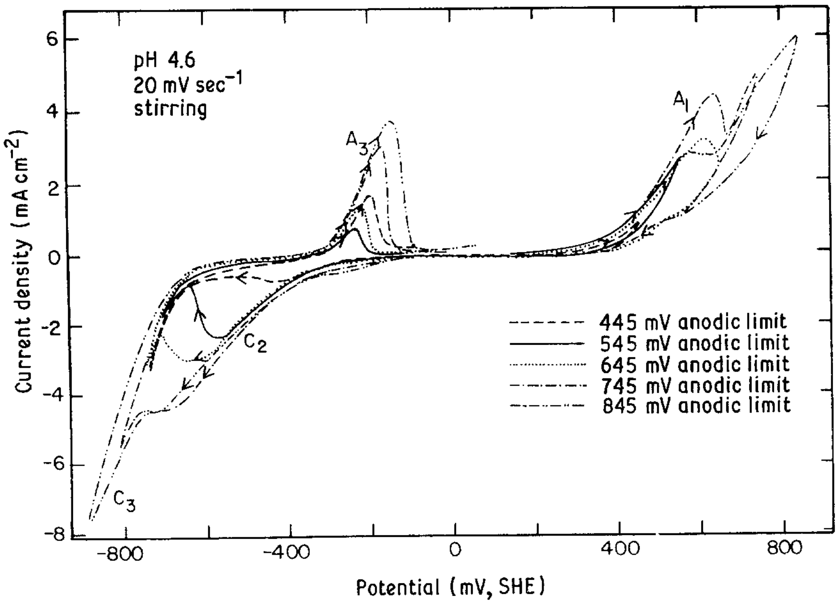

Fig. 3. Effect of the anodic limit on the single sweep voltammograms for a galena electrode immersed in a stirred 0.5 M CH_3COOH/0.5 M CH_3COONa solution (pH 4.6). Scan rate = 20 mV sec^{-1}.

A_1 = PbS, $CH_3COO^-/Pb(CH_3COO)_2$, S^0
A_3 = Pb^0, $CH_3COO^-/Pb(CH_3COO)_2$
C_2 = S^0/H_2S
C_3 = PbS/Pb^0, H_2S

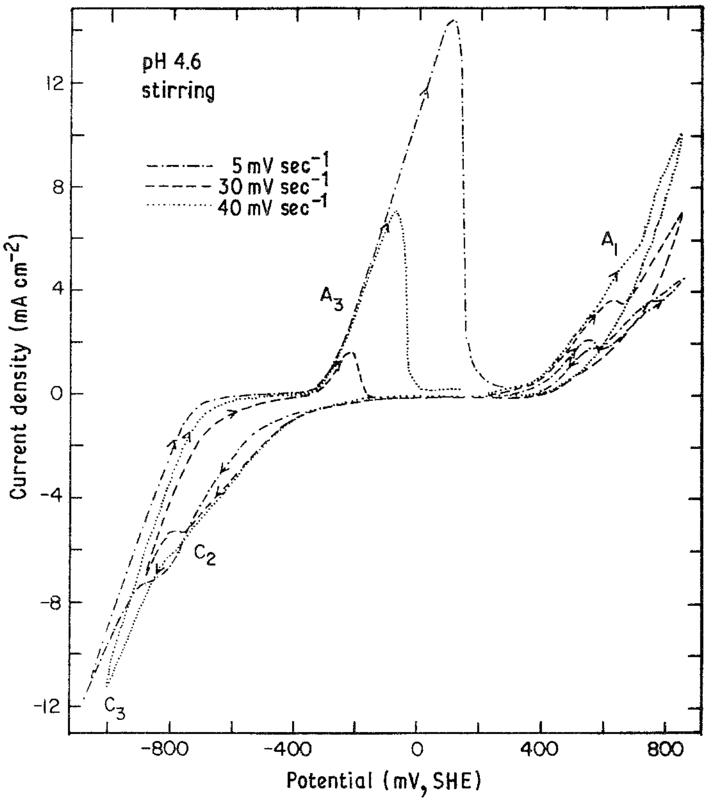

Fig. 4. Effect of scan rate on the single sweep voltammograms for a galena electrode immersed in a stirred 0.5 M CH_3COOH/0.5 M CH_3COONa solution (pH 4.6).

A_1 = PbS, $CH_3COO^-/Pb(CH_3COO)_2$, S^0
A_3 = Pb^0, $CH_3COO^-/Pb(CH_3COO)_2$
C_2 = S^0/H_2S
C_3 = PbS/Pb^0, H_2S

Although the amount of oxidation increases as the anodic limit is extended, the current rise from one test run to the next is not very reproducible, particularly once the potential reaches above about 500 mV. It should be pointed out that electrodeposition and electrodissolution processes are inherently stochastic in nature. Variations in the state of the galena surface prior to each test and in the formation and growth of sulphur nuclei during the potential sweep may contribute to some of the non-reproducibility.

The integrated charges show that even at a potential as high as 845 mV, there is still a balance between the anodic and cathodic charges. This indicates that $S_2O_3^{2-}$ or SO_4^{2-} are not readily produced by the oxidation of galena at pH 4.6.

3.3. *Effect of scan rate*

The effect of scan rate has also been investigated and the resulting voltammograms and integrated charges are presented in Fig. 4 and Table 3. For the most part, increasing the scan rate increases the current densities. Furthermore, it tends to smooth out the maximum at about 600–650 mV during the anodic rise and shift it toward higher potentials.

It is not possible to separate the reduction of the oxidation products from that of the mineral itself on these curves. As has been done previously, the anodic peak, A_3, due to the oxidation of Pb^0 to $Pb(CH_3COO)_2$, has been included in the charge analysis to determine how much of the cathodic charge can be attributed to C_2. (It should be noted that C_1 does not appear since the electrolyte is being stirred in this experiment.) The results of this analysis, given in Table 3, show that Q_{C_2} remains equivalent to Q_{A_1} regardless of the scan rate. Evidently, A_1 and C_2 can still be associated with reactions (2) and (4), respectively. The almost exact charge balance also strengthens the assumption that all the Pb^0 generated by the reduction of galena at this pH is removed by the oxidation process at A_3.

Table 3. The effect of scan rate on the anodic and cathodic charges at pH 4.6

Scan rate (*mV sec*$^{-1}$)	Q_{A_1} (*mC cm*$^{-2}$)	$Q_{C_2+C_3}$ (*mC cm*$^{-2}$)	Q_{A_3} (*mC cm*$^{-2}$)	Q_{C_2} (*mC cm*$^{-2}$)
5	424.1	1123.1	701.9	421.2
10	237.1	457.9	218.8	239.1
20	118.8	142.1	23.6	118.5
30	90.0	89.5	5.2	84.3
40	94.3	124.5	29.0	95.5
50	67.1	76.2	7.4	68.8

The data in Table 3 also show that while the current density during the anodic sweep increases with scan rate, the amount of charge passed steadily diminishes. One reason for this behavior may be that the faster the potential is swept, the higher the initial rate of deposition and the less porous and more passivating the sulphur film becomes. Another reason may be that dissolution of galena is not rapid enough to keep up with the decrease in time permitted for oxidation as the sweep rate increases.

Another interesting observation concerning the voltammograms in Fig. 4 is that at the slowest speed (5 mV sec^{-1}), the current is greater during the negative-going portion of the anodic scan than during the positive-going part. This phenomenon is characteristic of nucleation and growth processes and has been observed by others [13, 15] for the galena system at

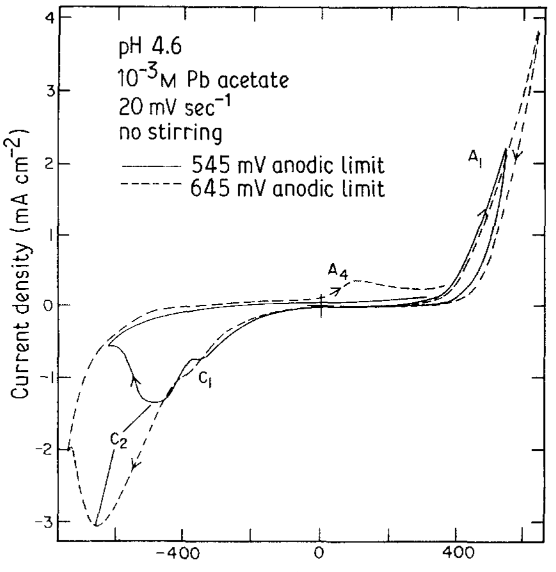

Fig. 5. Effect of anodic limit on the single sweep voltammograms for a galena electrode immersed in an unstirred 0.5 M CH_3COOH/0.5 M CH_3COONa solution (pH 4.6) + 10^{-3} M lead acetate solution. Scan rate = 20 mV sec^{-1}.

A_1 = PbS, CH_3COO^-/$Pb(CH_3COO)_2$, S^0
A_4 = H_2S/S^0
C_1 = $Pb(CH_3COO)_2$, S^0/PbS, CH_3COO^-
C_2 = S^0/H_2S

pH 1.1. At higher scan rates, however, the current is greater on the forward scan than on the backward scan. Gardner and Woods [15] also found that scan rate has a similar effect from their work at pH 1.1. It is difficult to say whether the dissolution mechanism changes as the scan rate is raised or whether a single process (presumably nucleation and growth), which manifests itself differently at low and high scan rates, is occurring.

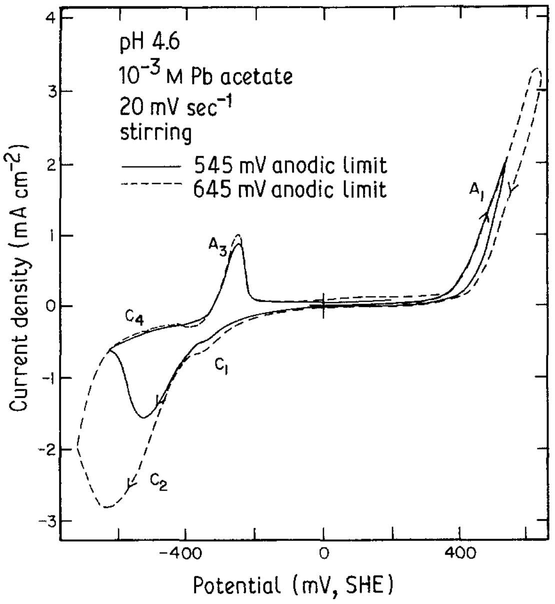

Fig. 6. Effect of anodic limit on the single sweep voltammograms for a galena electrode immersed in a stirred 0.5 M CH_3COOH/0.5 M CH_3COONa solution (pH 4.6) + 10^{-3} M lead acetate solution. Scan rate = 20 mV sec^{-1}.

A_1 = PbS, CH_3COO^-/$Pb(CH_3COO)_2$, S^0
A_3 = Pb^0, CH_3COO^-/$Pb(CH_3COO)_2$
C_1 = $Pb(CH_3COO)_2$, S^0/Pbs, CH_3COO^-
C_2 = S^0/H_2S
C_4 = $Pb(CH_3COO)_2/Pb^0$, CH_3COO^-

3.4. *Effect of dissolved lead concentration*

In a typical industrial leaching situation where the surface area of the galena is as high as is feasible, there will be a gradual build-up of the dissolved lead concentration as the process continues. Consequently, it is important to study the effect of dissolved lead upon the solution chemistry of galena. Accordingly, experiments have been conducted in 10^{-3} and 10^{-2} M lead acetate solutions.

Figs 5 and 6 show current-potential curves for anodic limits of 545 and 645 mV obtained in both unstirred and stirred 10^{-3} M lead acetate solutions. The addition of lead appears to have several important consequences. Comparison of the current densities with those in Fig. 2 indicates that the oxidation rate of galena is lowered in the presence of soluble lead ions. This is consistent with what has previously been reported by Paul *et al.* [13].

A second observation is that stirring no longer increases the anodic current, regardless of whether the potential is swept up to 545 or 645 mV. In these experiments, the surface concentration of soluble lead will always be quite high whether the solution is stirred or not. It is possible that, at such levels, the effects of concentration polarization become less important and consequently stirring no longer has much of an effect on the oxidation rate. Another effect of the presence of dissolved lead is that the C_1 peak appears in both stirred and unstirred cases. This provides further support that this peak should be identified with the reaction between $Pb(CH_3COO)_2$ and S^0 to form PbS (i.e., reaction (3)).

Once the lower potential limit is reached and the scan direction is reversed, there is a difference in the behavior of the current in the potential range from −550 to −200 mV, depending on whether the solution is being stirred or not. In the case of a stagnant solution (Fig. 5), little cathodic current flows from approximately −550 to −330 mV and the A_3 peak does not appear once the scan is reversed back in the anodic direction. However, when the solution is agitated (Fig. 6), a virtually constant current density of about −0.4 mA cm^{-2} is observed until about −330 mV, whereupon the current rises sharply to form the A_3 peak. There are several reasons to believe that the elemental lead being oxidized at A_3 does not originate from the reduction of galena, but from a cathodic reaction, C_4, occurring from −550 to −330 mV on the second anodic-going sweep. For one thing, measurement of the charges associated with the anodic and cathodic current rises on the voltammograms in Figs 5 and 6 shows that by the time the lower potential limit is reached, galena reduction has not yet occurred to an appreciable extent. For another, the amount of charge associated with the A_3 peak ($\sim$ 1.2 mC) is quite close to the amount estimated to pass between −550 and −330 mV.

The most likely cathodic reaction that occurs at C_4 is the reduction of the added lead to the elemental form. In the presence of acetate, the reaction is presumably

$$Pb(CH_3COO)_2(aq) + 2e \longrightarrow Pb^0 + 2CH_3COO^- . \qquad (9)$$

It is also significant that the current signal for this reaction is noisy when the solution is being stirred. This is indicative of a reaction that is diffusion-controlled. Stirring, which in these experiments was done with a magnetic bar, will continually replenish the $Pb(CH_3COO)_2$ at the electrode, resulting in a current that, on the average, is constant but periodically fluctuates. The absence of the A_3 peak in the unstirred case indicates that little or no deposition has taken place. Apparently, the supply of lead to the mineral surface is not fast enough to sustain the reaction at an appreciable rate.

To further check the validity of assigning reaction (9) to A_3, it is important to compare the Nernst potential for this reaction with the position of A_3 in the voltammogram. However, this is complicated by the fact that it is necessary first to calculate the equilibrium concentrations of the various complexes that result when lead acetate is dissolved in the acetate solution. We do this by setting up the following mass balance equations for lead and acetate:

$$[Pb^{2+}] + [PbCH_3COO^+] + [Pb(CH_3COO)_2] + [Pb(CH_3COO)_3^-] + [Pb(CH_3COO)_4^{2-}] = [Pb]_{in} \qquad (10)$$

$$[CH_3COO^-] + [CH_3COOH] + [PbCH_3COO^+] + 2[Pb(CH_3COO)_2] + 3[Pb(CH_3COO)_3^-] + 4[Pb(CH_3COO)_4^{2-}] = [Ac]_{in} \qquad (11)$$

where $[Pb]_{in}$ and $[Ac]_{in}$ are the total amount of lead and acetate, respectively, added to the system. The concentrations of the various species are related through equilibria of the type

$$Pb^{2+} + nCH_3COO^- = Pb(CH_3COO)_n^{2-n} \quad (n = 1, \ldots, 4), \qquad (12)$$

from which we obtain,

$$[Pb(CH_3COO)_n^{2-n}] = \frac{\gamma_{Pb^{2+}} \cdot (\gamma_{CH_3COO^-})^n}{\gamma_{Pb(CH_3COO)_n^{2-n}}} \times K_n[Pb^{2+}][CH_3COO^-]^n \qquad (13)$$

where K_n is the equilibrium constant for reaction (12). The values of these constants can be determined from the free energy data in Table 1. The relation between $[CH_3COO^-]$ and $[CH_3COOH]$ is dictated by the reaction,

$$CH_3COO^- + H^+ = CH_3COOH \qquad (14)$$

Table 4. Equilibrium concentration of species in lead/acetate system containing 10^{-3} M lead acetate dissolved in 0.5 M CH_3COOH/0.5 M CH_3COONa electrolyte at pH 4.6

Species	*Concentration (M)*
CH_3COO^-	0.5
CH_3COOH	0.5
Pb^{2+}	1.91×10^{-6}
$PbCH_3COO^+$	1.04×10^{-4}
$Pb(CH_3COO)_2$	6.26×10^{-4}
$Pb(CH_3COO)_3^-$	2.43×10^{-4}
$Pb(CH_3COO)_4^{2-}$	2.54×10^{-5}

and the corresponding condition,

$$[CH_3COOH] = \frac{\gamma_{CH_3COO^-}}{\gamma_{CH_3COOH}} K_a a_{H^+}[CH_3COO^-] \qquad (15)$$

where K_a is the equilibrium constant for (14). By combining equations (10), (11), (13) and (15) using the Davies equation (1) for the activity coefficients, we can reduce the problem to a single algebraic equation in one unknown (see Appendix I). This can then be solved numerically for particular values of pH, $[Pb]_{in}$ and $[Ac]_{in}$ to yield the concentrations of the various species.

Table 4 shows the equilibrium concentrations that have been obtained for the case which matches the experimental conditions of Fig. 6, i.e., 10^{-3} M lead acetate initially dissolved in the 0.5 M CH_3COOH/0.5 M CH_3COONa electrolyte at pH 4.6. Using the values of $[CH_3COO^-]$ and $[Pb(CH_3COO)_2]$ from this table and γ_{CH_3COO} and $\gamma_{Pb(CH_3COO)_2}$ from the Davies equation, we calculate the Nernst potential for reaction (9) to be −314 mV. This is in excellent agreement with the potential where the peak at A_3 begins to rise in Fig. 6.

It is interesting to compare the reversible potential that has just been calculated with the value obtained without taking into account any possible complex formation between lead and acetate. In the absence of any complexes, the logical choice for the anodic reaction at A_3 is

$$Pb^0 \longrightarrow Pb^{2+} + 2e \qquad (16)$$

Furthermore, all of the dissolved lead added to the electrolyte will be present in the form of Pb^+ ions. We find under such circumstances that the Nernst potential for reaction (16) is −234 mV. This value is much farther from the front edge of A_3 than is the potential calculated for reaction (9). Equally important is the fact that it lies far on the *anodic* side of the front edge. This would mean that the process associated with A_3 is occurring with a substantial, but rather unlikely, underpotential. This lends further support to the idea that the process of A_3 is more likely to occur via a reaction such as (9) which involves a lead acetate complex.

The results of the voltammogram for 10^{-3} M lead acetate in Fig. 6 can be used to estimate the diffusion boundary layer thickness for the deposition of lead onto galena. Assuming that the process is entirely mass transfer-controlled and that the boundary layer thickness remains constant, then the limiting current density, i_d, for the deposition can be expressed as:

$$i_d = \frac{nFDC^*}{\delta} \qquad (17)$$

where n = number of electrons transferred
F = Faraday constant
D = diffusion coefficient of $Pb(CH_3COO)_2$
C^* = bulk $Pb(CH_3COO)_2$ concentration
δ = diffusion boundary layer thickness.

This equation can be used to calculate δ once i_d, n, D and C^* are known. In this case, n and C^* are equal to 2 and 6.26×10^{-4} M, respectively. Diffusion coefficients for ions in aqueous solutions are typically on the order of $10^{-5}\,cm^2\,sec^{-1}$ [20]. A value of $0.4\,mA\,cm^{-2}$ can be estimated for i_d on the basis of the constant current density obtained for the deposition of lead from the voltammogram in Fig. 6. Substituting these parameters into equation (17), $\delta \sim 3 \times 10^{-3}$ cm is obtained. Diffusion-layer thicknesses determined experimentally typically range from 10^{-5} to 10^{-2} cm depending on the rate of agitation [21]. Considering that stirring during these experiments was carried out using a magnetic stirrer and was not too vigorous, the value of δ estimated here is reasonable.

It is also interesting to note that the deposition of lead only begins after the elemental sulphur oxidation product is removed during the cathodic-going scan. Since sulphur is passivating, the soluble lead would have to diffuse through this layer to the unreacted PbS core in order to be reduced to the metallic form. This process is certain to be slow and, consequently, will only commence once the oxidation products have been removed.

Another possible reason for this behaviour may be that as the elemental sulphur is being reduced during the cathodic scan (i.e., reaction (4)), the H_2S that is generated reacts with incoming $Pb(CH_3COO)_2$ to form PbS, i.e.,

$$Pb(CH_3COO)_2 + H_2S \longrightarrow PbS + 2H^+ + 2CH_3COO^- . \qquad (18)$$

This reaction is thermodynamically possible since its free energy change is negative under the conditions of these experiments. Since it does not involve the transfer of any electrons, its effect on the electrode response will not show up directly as a flow of current. However, the role reaction (18) may play is to consume enough $Pb(CH_3COO)_2$ that deposition of lead by reaction (9) is not possible. Only once all the elemental sulphur is removed and H_2S is no longer being produced will deposition begin to occur.

In order to look more closely at the effect of the state of the mineral surface on the deposition of elemental lead on galena, voltammograms were obtained both in the presence and absence of 10^{-3} M lead acetate when the limit during the first anodic-going scan was only 345 mV (Fig. 7). Comparison of these results with those in Fig. 6 clearly shows that the presence of oxidation products on galena suppresses deposition. When little or no oxidation is allowed to take place prior to reduction, elemental lead begins to be deposited as soon as the potential drops below about −300 mV during the cathodic-going scan. When the electrode is oxidized prior to the cathodic scan, deposition only begins after elemental sulphur has been removed from the surface.

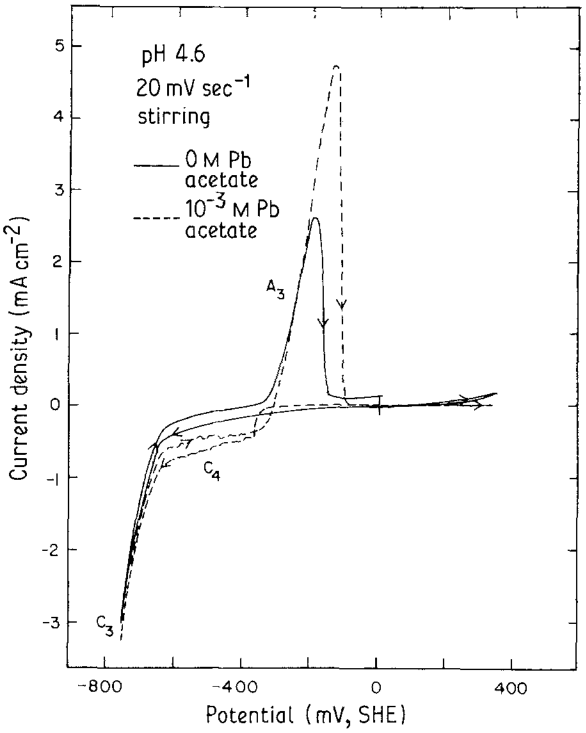

Fig. 7. Effect of lead acetate addition on the cathodic portion of the single sweep voltammograms for a galena electrode immersed in a stirred 0.5 M CH_3COOH/0.5 M CH_3COONa solution (pH 4.6) solution. Scan rate = $20\,mV\,sec^{-1}$.

A_3 = Pb^0, $CH_3COO^-/Pb(CH_3COO)_2$
C_3 = PbS/Pb^0, H_2S
C_4 = $Pb(CH_3COO)_2/Pb^0$, CH_3COO^-

It should also be noted that the reduction of galena itself commences at −600 mV no matter whether there is dissolved lead in solution or not. Apparently, the occurrence of reaction (9) does not interfere with reaction (5) at this Pb^{2+} concentration.

When the dissolved lead concentration is raised to 10^{-2} M, the results given in Fig. 8 are obtained. The oxidation of galena is not enhanced by agitation, similarly to what was found for 10^{-3} M lead acetate. Furthermore, the anodic current is essentially the same as at the lower lead concentration. Both these observations are consistent with the previous discussion that the bulk concentration of soluble lead is high enough that there might be no further inhibition of reaction (2).

With a reversal of the scan direction, the current-potential curves are drastically different from what has happened previously. The cathodic peak due to reaction (3) is observed at approximately −350 mV,

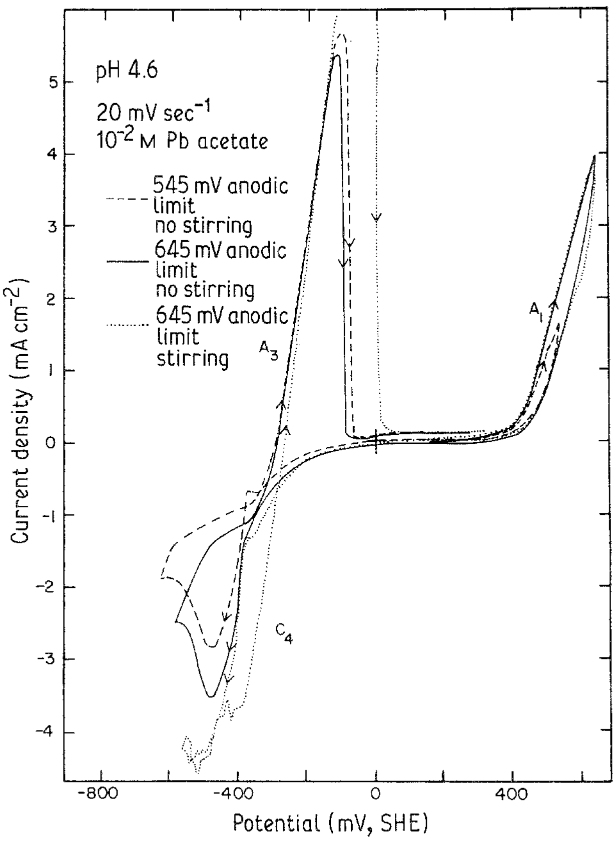

Fig. 8. Effect of anodic limit and stirring on the single sweep voltammograms for a galena electrode immersed in a 0.5 M CH_3COOH/0.5 M CH_3COONa (pH 4.6) + 10^{-2} M lead acetate solution. Scan rate = 20 mV sec^{-1}.

A_1 = PbS, $CH_3COO^-/Pb(CH_3COO)_2$, S^0
A_3 = Pb^0, $CH_3COO^-/Pb(CH_3COO)_2$
C_4 = $Pb(CH_3COO)_2/Pb^0$, CH_3COO^-

as in the case of 10^{-3} M lead, in all three voltammograms in Fig. 8. However, just beyond this, the cathodic current rises sharply, although in quite a different manner depending on whether the solution is stagnant or not. The current density in the stirred case is greater and displays a noisy signal as the potential drops below −400 mV. Also, when the potential is reversed back in the anodic-going direction, the current is greater than it is in the first direction. This behaviour is strongly suggestive of the diffusion-controlled deposition of lead under stirred conditions. Without stirring, the cathodic current increases to a maximum of about −500 mV before diminishing as the potential approaches the lower limit. The shape of these curves is very characteristic of that obtained for diffusion-controlled reactions under stagnant conditions. Further evidence that lead is being deposited is that there is a tremendous growth in the A_3 peak when the scan is reversed back in the anodic direction. These results contrast strongly with those obtained previously for a 10^{-3} M lead acetate addition in a quiescent solution (Fig. 5), where there was no evidence of any deposition. Apparently, at the higher lead level, the rate of transport of the reactant to the electrode is sufficient to permit deposition to occur at a measurable rate.

Another difference from what is observed at 10^{-3} M lead acetate is that the reduction of S^0 to H_2S at C_2 does not seem to occur as a step distinct from the deposition of lead. Evidently, at the higher lead level, deposition begins to occur before all the elemental sulphur has been removed. Once deposition begins, it is not obvious, however, whether the reduction of the oxidation products from the anodic scan still proceeds or is suppressed altogether.

4. Conclusions

The principal findings of this study of the electrochemistry of galena at pH 4.6 in an acetate solution can be summarized as follows:

1. Elemental sulphur is the only sulphur-bearing species produced during the anodic oxidation of galena, at least below a potential of 845 mV. Thermodynamic considerations suggest that the aqueous species, $Pb(CH_3COO)_2$, is the primary lead-bearing product formed.

2. The reduction of oxidation products occurs via two reactions under quiescent conditions, i.e., the recombination of $Pb(CH_3COO)_2$ and S^0 to PbS and the reduction of S^0 to H_2S. The first reaction contributes less than 20% of the cathodic charge. In agitated solutions, soluble lead species are dispersed away from the electrode and consequently only the second reaction occurs.

3. The addition of 10^{-3} or 10^{-2} M lead acetate to the electrolyte decreases the rate of anodic dissolution of galena.

4. When 10^{-3} or 10^{-2} M lead acetate is added to the electrolyte, deposition of lead on galena can occur when the potential is lowered below about −330 mV. At 10^{-3} M lead acetate, deposition only begins once all the elemental sulphur generated during oxidation has been removed. At 10^{-2} M, however, it can begin even when some of the oxidation product is still present on the mineral surface.

Acknowledgements

The authors express their gratitude to Dr Ron Woods for his valuable discussions, to the referees of this paper for their useful comments concerning the manuscript, and to Beth Dillinger for reading and typing the manuscript. They also acknowledge the financial support of the National Science Foundation (Grant No. CPE-8303860) and the Virginia Mining and Minerals Research Institute.

Appendix I

Derivation of algebraic equation used to solve mass balance equations

By substituting (13) into (10), we obtain the following expression for $[Pb^{2+}]$ in terms of $[CH_3COO^-]$:

$$[Pb^{2+}] = \frac{[Pb]_{in}}{\gamma_{Pb^{2+}} \sum_{n=0}^{4} \frac{(\gamma_{CH_3COO^-})^n}{\gamma_{Pb(CH_3COO)_n^{2-n}}} K_n [CH_3COO^-]^n} \tag{A1}$$

We can also write equation (11) in terms of $[\mathrm{Pb}^{2+}]$ and $[\mathrm{CH_3COO^-}]$ by using (13) and (15):

$$[\mathrm{CH_3COO^-}]\left(1 + \frac{\gamma_{\mathrm{CH_3COO^-}}}{\gamma_{\mathrm{CH_3COOH}}} K_\mathrm{a} \mathrm{a}_{\mathrm{H^+}}\right) + \gamma_{\mathrm{Pb^{2+}}}[\mathrm{Pb}^{2+}] \times \sum_{n=0}^{4} \frac{n(\gamma_{\mathrm{CH\,COO^-}})^n}{\gamma_{\mathrm{Pb(CH_3COO)}_n^{2-n}}} K_n[\mathrm{CH_3COO^-}]^n = [\mathrm{Ac}]_{\mathrm{in}} \tag{A2}$$

and then eliminate $[\mathrm{Pb}^{2+}]$ from (A2) with (A1) to yield:

$$\left(1 + \frac{\gamma_{\mathrm{CH_3COO^-}}}{\gamma_{\mathrm{CH_3COOH}}} K_\mathrm{a} \mathrm{a}_{\mathrm{H^+}}\right) \sum_{n=0}^{4} \frac{(\gamma_{\mathrm{CH\,COO^-}})^n}{\gamma_{\mathrm{Pb(CH_3COO)}_n^{2-n}}} \times K_n[\mathrm{CH_3COO^-}]^{n+1} + \sum_{n=0}^{4} (n[\mathrm{Pb}]_{\mathrm{in}} - [\mathrm{Ac}]_{\mathrm{in}}) \times \frac{(\gamma_{\mathrm{CH_3COO^-}})^n}{\gamma_{\mathrm{Pb(CH_3COO)}_n^{2-n}}} K_n[\mathrm{CH_3COO^-}]^n = 0 \tag{A3}$$

The activity coefficients are also functions of $[\mathrm{CH_3COO^-}]^n$ through their dependency on the ionic strength, I, in the Davies equation:

$$\log \gamma_\mathrm{i} = -Az_\mathrm{i}^2\left\{\frac{I^{1/2}}{1 + I^{1/2}} - 0.2I\right\} \tag{A4}$$

where

$$I = 1/2\{4[\mathrm{Pb}^{2+}] + [\mathrm{PbCH_3COO^+}] + [\mathrm{Pb(CH_3COO)_3^-}] + 4[\mathrm{Pb(CH_3COO)_4^{2-}}] + [\mathrm{CH_3COO^-}] + [\mathrm{Na^+}] + [\mathrm{H^+}]\} \tag{A5}$$

By combining (A4) and (A5) into (A3), we can solve the resulting equation iteratively for $[\mathrm{CH_3COO^-}]$, given a particular set of $\mathrm{a_{H^+}}$, $[\mathrm{Pb}]_{\mathrm{in}}$, $[\mathrm{Ac}]_{\mathrm{in}}$ and $[\mathrm{Na^+}]$. The equilibrium concentrations of the other species can then be calculated by substituting the value of $[\mathrm{CH_3COO^-}]$ back into equations (13) and (15).

References

[1] F. A. Forward and I. H. Warren, *Met. Rev.* **5** (1960) 137.

[2] G. C. Bratt and R. W. Pickering, *Met. Trans.* **1** (1970) 2141.

[3] H. R. Skewes, *Proc. Aust. Inst. Min. Met.* **244** (1972) 35.

[4] P. E. Queneau and R. Schuhmann, *J. Metals* **26** (1974) 14.

[5] D. Morin, A. Gaunand and H. Renon, *Metall. Trans.* **16** (1984) 31.

[6] J. E. Dutrizac, Presented at the 114th AIME Annual Meeting, New York, February, 1985.

[7] M. K. Han and M. E. Wadsworth, *ibid.*

[8] J. Perez, *Geomimet* **135** (1985) 48.

[9] J. E. Murphy, B. R. Eichbaum and J. A. Eisele, *Miner. Metall. Process.* **2** (1985) 38.

[10] J. B. Brodie, Electrochemical Dissolution of Galena. M.Sc. Thesis, University of British Columbia, Vancouver, British Columbia, Canada, 1969.

[11] P. Eadington and A. P. Prosser, *Trans. IMM* **78** (1969) C74.

[12] G. Springer, *ibid.* **79** (1970) C11.

[13] R. L. Paul, M. J. Nicol, J. W. Diggle and A. D. Saunders, *Electrochim. Acta* **23** (1978) 625.

[14] J. W. Johnson, J. Chang, R. A. Narasagoudar and T. J. O'Keefe, *J. Appl. Electrochem.* **8** (1978) 25.

[15] J. R. Gardner and R. Woods, *J. Electroanal. Chem.* **100** (1979) 447.

[16] M. Lamache, D. Bauer and J. Pegouret, *Electrochim. Acta* **26** (1981) 1845.

[17] P. Sivenas and F. R. Foulkes, *ibid.* **29** (1984) 1215.

[18] A. E. Martell and R. M. Smith, *Critical Stability Constants. Organic Ligands*, Vol. 3. Plenum Press, New York (1977) 6.

[19] T. R. Blackburn, *Equilibrium. A Chemistry of Solutions.* Holt Rinehart, New York (1969) 187.

[20] G. H. Geiger and D. R. Poirier, *Transport Phenomena in Metallurgy.* Addison-Wesley, Reading, Massachusetts (1973) 463.

[21] L. I. Antropov, *Theoretical Electrochemistry* (English Translation). Mir Publishers, Moscow (1972) 329.